CHARACTERIZATION OF HIGH-POWER RF STRUCTURES USING TIME-DOMAIN FIELD CODES *

C. C. Shang, J. F. DeFord, and T. L. Swatloski
Lawrence Livermore National Laboratory, L-440, Livermore, CA 94550

Abstract

We have modeled gyrotron windows and gyrotron amplifier sever structures for TE modes in the 100-150 GHz range and have computed the reflection and transmission characteristics from the field data. Good agreement with frequency domain codes and analytic analysis have been obtained for some simple geometries. We present results for realistic structures with lossy coatings and describe implementation of microwave diagnostics.

Introduction

The use of high-power microwaves to heat the plasma in an MFE reactor at the electron-cyclotron resonance can yield a number of benefits, including bulk-heating and preionization of the plasma, reaction startup, and instability suppression. The use of electron-cyclotron heating (ECH) in tokamak and stellerator reactors has been studied in many significant MFE experiments, including C-mod at MIT and DIII-D at General Atomics in the U.S.; Compass at Culham, England; T-10 at the Kurchatov Institute, Russia; and the Heliotron at Nagoya, Japan.

Operating parameters of interest for ECH applications include frequencies in the 140-250 GHz range and output power in the vicinity of 1 MW per bottle [1]. Currently, the fixed-frequency, mm-wave source available for use in the 1 MW range is the gyrotron. Understanding of the microwave properties of high-average-power RF structures is crucial to the design of gyrotron tubes and amplifier devices. Dissipation of the RF (ohmic loss) and excessive mode conversion are often limiting factors in the performance and robustness of the overall device. These issues and others pertaining to mm-wave devices may be investigated using time domain EM field codes [2]. An advantage of simulation in the time domain is that EM characteristics may be obtained over a wide bandwidth from a single calculation. Excitation of the frequencies of interest may be obtained by launching modulated pulses driven by magnetic currents. A general field code such as AMOS [3] may be used to launch the prescribed modes at the frequency or frequencies of interest to examine mm-wave component performance by exact numerical integration of the Maxwell equations.

Mode Launching

Gyrotron oscillators operate with whispering gallery (WG) modes (radial mode number >> axial mode number). Thus, most of the RF is distributed near the beampipe wall. As the mode propagates near the window, the modes couple into the perturbation in the wall, leading to mode conversion. To model gyrotron components requires the launching of transverse electric ($TE_{n,m}$) modes. This may be accomplished by driving magnetic currents over the beampipe aperture.

In order to describe the location of the TE drive-nodes, we rewrite the EM time dependent curl equations

$$\nabla \times \vec{H} = \sigma \vec{E} + \epsilon \frac{\partial \vec{E}}{\partial t} + \vec{J}_s \tag{1}$$

$$\nabla \times \vec{E} = -\mu \frac{\partial \vec{H}}{\partial t} - \vec{K}_s \tag{2}$$

in the integral form

$$\oint \vec{H} \bullet d\vec{\ell} = \int\int \left(\sigma \vec{E} + \epsilon \frac{\partial \vec{E}}{\partial t} + \vec{J}_s\right) \bullet d\vec{A} \tag{3}$$

$$\oint \vec{E} \bullet d\vec{\ell} = -\int\int \left(\mu \frac{\partial \vec{H}}{\partial t} + \vec{K}_s\right) \bullet d\vec{A} \tag{4}$$

K source components are co-located with H field components on the Yee lattice [4]. Referring to figure 1 and equation 4, one can see that driving the K_r component of the magnetic current will excite the proper H_r, H_z and E_ϕ fields. Similarly, K_ϕ currents excite E_r, and H_ϕ field components. E_z induced by K_ϕ and K_r cancels out.

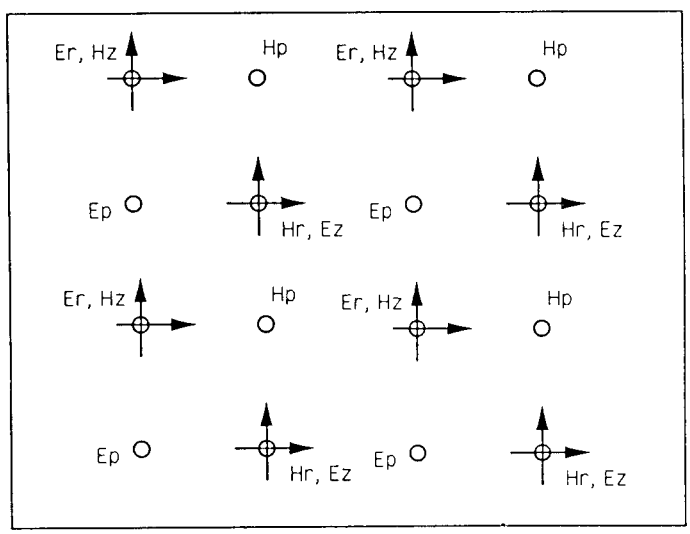

Fig. 1. TE Drive-Node Location on the Yee Lattice.

The proper spatial variation of magnetic currents required to obtain propagating WG $TE_{22,2}$ modes are the Bessel function $J_{22}(x)$ out to the second zero, and its

* Work performed under the auspices of the U. S. Department of Energy by LLNL under contract W-7405-ENG-48.

derivative $J'_{22}(x)$ which directly drive K_ϕ and K_r, respectively. The amplitude distribution in time, can be a modulated pulse to obtain the required frequency content.

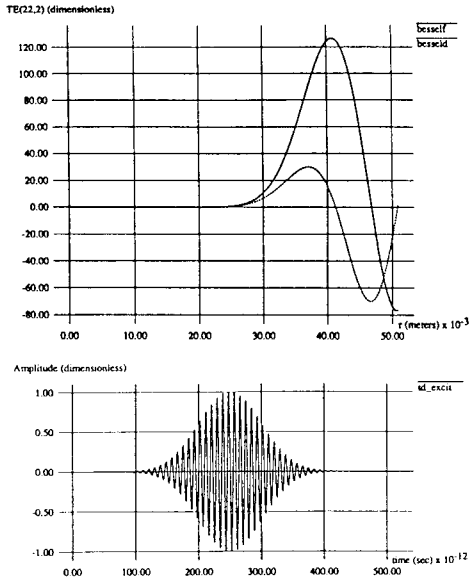

Fig. 2. Launching $TE_{22,2}$ Whispering Gallery Mode - Spatial and Temporal Magnetic Drive Function.

Field diagnostics for computing the voltage standing wave ratio (VSWR) were incorporated into AMOS by sampling electric fields at "numerical" probes and computing the VSWR directly from the field values. If $\mathcal{F}[f(t)]$ denotes the forward Fourier transform, then the VSWR may be computed from the field data by first computing the reflection coefficient (no mode conversion)

$$\Gamma = \sqrt{1.0 - (|\frac{\mathcal{F}[e_{smp}(t)]}{\mathcal{F}[p_{mod}(t)]}|)^2} \qquad (5)$$

where $e_{smp}(t)$ is the sampled electric field on the "downstream" side of the window and $p_{mod}(t)$ is the modulated pulse in time. The VSWR is computed according to the definition $VSWR = (1.0 + \Gamma)/(1.0 - \Gamma)$.

High-Power RF Window Analysis

Presently, gyrotrons operate in the 100-150 GHz and ~1 MW regime. Future performance requirements will increase power levels to the multi-megawatt range with frequencies approaching 250 GHz. In this scenario, several gyrotron components will be placed under severe mechanical and thermal stress. Until now, less demanding performance constraints have rendered non-ideal component effects less important. However, understanding these effects is now critical to the operation of the device. We now examine high-order mode scattering caused by various RF window geometries at the exit of the gyrotron. The VSWR associated with the window can be determined over a broad spectrum of frequencies using data from a single time-domain run using the technique described in the previous section.

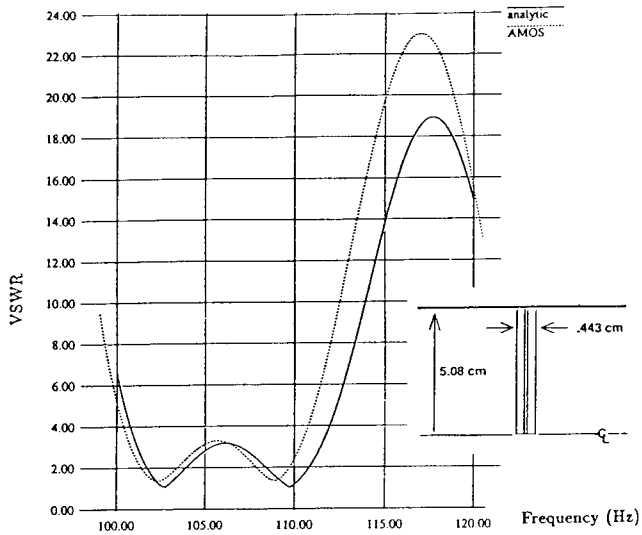

Fig. 3. VSWR for idealized 110 GHz bandpass, RF window compared to theory.

In Figure 3, we find good agreement between AMOS and analytic values [5] for the VSWR of a three-layer RF window. The gyrotron window geometry includes a beampipe radius of 5.08 cm with the longitudinal extent of the window at 0.443 cm. The window material has $\epsilon_r = 9.387$ and the dielectric cooling fluid has $\epsilon_r = 1.797$. A small difference between the AMOS and frequency code results is evident, caused by a minor variation in window element thicknesses resulting from the use of a regular grid in AMOS.

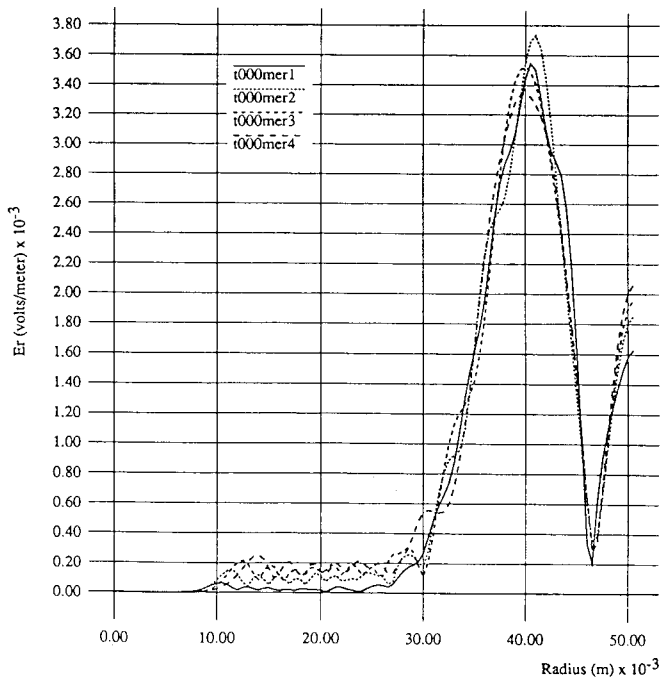

Fig. 4. Radial Field Profile at Varying Longitudinal Location for Realistic Gyrotron RF Window Structures.

The gyrotron window structure is grown from a sapphire crystal. These microwave components are often quite

expensive and difficult to fabricate, and more realistic window geometries cannot be easily treated analytically. In figure 4, a realistic window structure with the "coolant reservoir" is modeled. Compared to the idealized window, the electric fields near axis highlight coupling to modes through the RF window near the beampipe wall. At the multi-megawatt range, this amount of RF may be significant. However, the exact level of power per mode awaits further analysis.

Gyrotron Amplifier Sever

We performed a second set of calculations in which wave propagation through a microwave sever - a device for stopping or absorbing microwave energy while allowing a charged particle beam to pass undisturbed - is examined. Of interest is the understanding of the absorption in the lossy dielectric insert (see Figure 5) for a variety of lossy RF mixtures. The beampipe radius is 0.95 mm - operating near cutoff. As before, TE_{11} modes were launched by driving magnetic currents at the sever aperture. The material conductivity characteristics for 5 berrylia mixtures were obtained from the available experimental data at 12 GHz. Two materials, berrylia 80/20 and berrylia 60/40 are representative. The dielectric constant K' for berrylia 60/40 and 80/20 were 49.54 and 17.81 and the loss tangent 0.72 and 0.22, respectively [6].

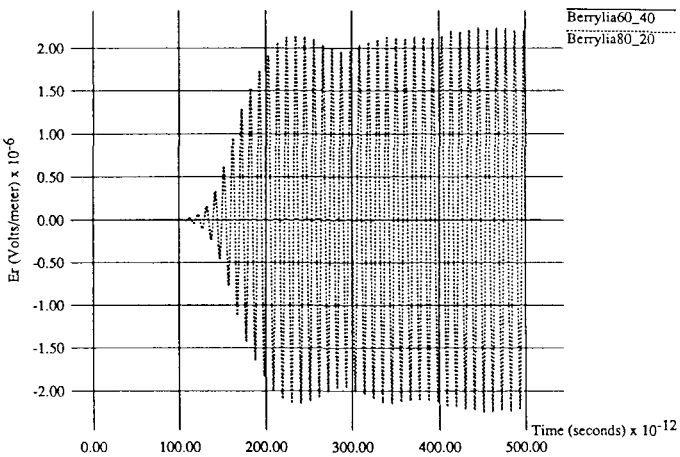

Fig. 5. Sever Performance for Berrylia 60/40 and 80/20.

AMOS predicted ~40 dB attenuation for a 95-GHz, TE_{11} mode propagating toward the sever for the berrylia 60/40 mixture. In comparison, unacceptably low RF absorption characteristics for the other berrylia mixtures (Figure 5) was evident. In the limit, when the conductivity is large (berrylia 60/40), the relevant diameter is not that of the beampipe but instead it is the diameter inside the sever section. With cutoff given by $\lambda_c = 2\pi a/1.84$, a TE_{11} mode at 95 GHz is well below cutoff, and the fields will be attenuated. This set of calculations can be repeated when updated berrylia measurements in the ~100 GHz range is available (MIT). For the previous class of modeling problem, we plan to examine simulation issues such as the launching of waveguide modes near cutoff. Further, the taper of the lossy section was initially limited to minimum of 5 degrees because of numerical limitations of a shallow-angle staircasing of the mesh. The conforming mesh algorithm in CG-AMOS [7] will allow exact boundary representation, and thus any shallow taper.

Conclusions

We have applied time-domain field codes to the analysis of mm-wave components. The proper TE modes may be launched in a beampipe by use of the dual K term (magnetic current) in the Faraday-Maxwell equation. TM modes may be launched using the similar dual technique. In the future we plan to use conforming grid codes to model output couplers. Some of the future work will also involve the use of unstructured meshes to simulate the important aspects of high-bandwidth RF window by detailed modeling of curved window surfaces and materials. We will also implement the diagnostics that will derive mode information directly from the field data.

Acknowledgements

We wish to thank Dr. M. Caplan (LLNL) for suggesting this set of modeling problems as well as for numerous helpful discussions. Stimulating discussions with Dr. W. DeHope of Varian and support and encouragement from Dr. F. Coensgen (LLNL) are gratefully acknowledged.

References

1. W. H. Urbanus, R. W. B. Best, A. G. Verhoeven, M. J. van der Wiel, FOM-Instituut voor Plasmafysica, Nederland, M. Caplan, Lawrence Livermore National Laboratory, USA, V. Bratman and G. Denisov, Institute of Applied Physics, Russia and A. A. Varfolomeev, Kurchatov Institute, Russia, "A 1 MW Free Electron Maser for Fusion Application," *Third European Particle Accelerator Conference,* Berlin, 24-28 March 1992.
2. M. Caplan, "Application of AMOS Code to Design of Complex Structures for Selective Microwave Absorption and Transmission," UCRL-ID-1099254, December 1991.
3. J. F. DeFord, G. D. Craig, and R. R. McLeod, "The AMOS Wakefield Code," in *Proceedings of the Conference on Computer Codes and the Linear Accelerator Community*, Los Alamos, New Mexico, Jan. 22-25, 1990, pages 265-289.
4. K. S. Yee, "Numerical Solution of Initial Boundary Value Problems Involving Maxwell's Equations in Isotropic Media," *IEEE Transactions on Antennas and Propagation.* Volume AP-14, May 1966, pages 302-307.
5. J. M. Nielsen, P. E. Latham, M. Caplan, and W. G. Lawson, "Determination of the resonant frequencies in a complex cavity using the scatter matrix formulation," *IEEE Transactions on Microwave Theory and Techniques,*" 37, August 1989, pp. 1165-1170.
6. W. DeHope, private communication, April 1992.
7. C. C. Shang and J. F. DeFord, "Modified-Yee Field Solutions in the AMOS Wakefield Code," *Proceedings of the 1990 Linear Accelerator Conference,* Albuquerque, NM, September 1990.